

2010-11

# ZnTe nanocrystal formation and growth control on UV-transparent substrate

Chemical Physics Letters,Amsterdam : Elsevier,v. 500, n. 1/3, p.46-48, Nov. 2010
http://www.producao.usp.br/handle/BDPI/49977

Chemical Physics Letters 500 (2010) 46–48

Contents lists available at ScienceDirect

Chemical Physics Letters

journal homepage: www.elsevier.com/locate/cplett

# ZnTe nanocrystal formation and growth control on UV-transparent substrate

Noelio Oliveira Dantas [a,*], Alessandra dos Santos Silva [a], Sebastião William da Silva [b], Paulo César de Morais [b], M.A. Pereira-da-Silva [c,d], Gilmar Eugênio Marques [e]

[a] Laboratório de Novos Materiais Isolantes e Semicondutores (LNMIS), Instituto de Física, Universidade Federal de Uberândia, CEP 38400-902 Uberdândia, Minas Gerais, Brazil
[b] Universidade de Brasília, Instituto de Física, Núcleo de Física Aplicada, CEP 70910-900 Brasília, DF, Brazil
[c] Instituto de Física de São Carlos – USP, CEP 13560-250 São Carlos, SP, Brazil
[d] Centro Universitário Central Paulista – UNICEP, CEP 13563-470 São Carlos, SP, Brazil
[e] Universidade Federal de São Carlos, Departamento de Física, 13560-905 São Carlos, SP, Brazil

ARTICLE INFO

*Article history:*
Received 26 July 2010
In final form 14 September 2010
Available online 17 September 2010

ABSTRACT

ZnTe nanocrystals (NCs) were successfully grown in a UV transparent, vitreous substrate synthesized by fusion and then annealed. The formation of dot structures, emitting in the UV-range, was investigated by optical absorption (OA), atomic force microscopy (AFM) and Raman spectroscopy. Dot growth was evidenced by an OA band red-shift with increasing annealing time. Average sizes of the ZnTe dots were determined using the effective mass fit model with OA spectra and comparing the results with estimates from AFM images. A UV-transparent PZABP vitreous matrix was used because it allowed ZnTe NC growth and displayed typical Raman active phonon modes.



## 1. Introduction

The II–VI semiconductor family, based on zinc telluride (ZnTe), has a zincblend crystalline structure with an exciton Bohr radius of 5.2 nm [1]. Due to its wide energy gap (2.26 eV) at room temperature [2–5], ZnTe is attractive for the manufacture of optoelectronic devices such as light emitting diodes, green-range laser diodes [6,7], electrochemical solar photocells [8,9] and efficient, phosphorus based displays. ZnTe has also attracted much attention because of its very high electro-optic coefficient and dielectric constant in the terahertz range – properties which can be advantageous as electro-optic field detectors [4,6,9,10]. Until now, ZnTe nanostructures have been synthesized by different techniques such as thermal evaporation, hot wall evaporation, radio frequency cathodic evaporation, solvothermal processes, molecular beam epitaxy [2,6,11–13] and colloidal solutions [5,14]. Most of these ZnTe structures have been obtained in the form of monocrystalline nanowires [6,9] and, more recently, nanocrystals [5]. Interest in NC band-gap is mainly due to its quantum confinement effect which is strongly dependent on NC size [15]. This study shows, probably for the first time, clear evidence of ZnTe nanocrystal growth in a vitreous matrix synthesized by fusion.

## 2. Experimental details

### 2.1. Sample preparation

ZnTe NC growth was detected after lengthy manipulation of the PZABP matrix yielding a UV-transparent template with final nominal composition: $65P_2O_5{\cdot}14ZnO{\cdot}1Al_2O_3{\cdot}10BaO{\cdot}10PbO$ (mol%), with homogenized and weighed 1Te (wt.%). Standard sample preparation procedures were followed that included mixing and fusing powder at 1300 °C for 30 min and then quickly cooling the melt to room temperature. To obtain different sized NCs, the samples underwent annealing at 480 °C for different time periods (2, 4, 6 and 8 h). Annealing not only favored controlled diffusion of $Zn^{2+}$ and $Te^{2-}$ ions but also stimulated the nucleation and growth of ZnTe NCs in the manipulated PZABP template. Average dot size was proportional to annealing time.

### 2.2. Instrumentation

OA spectra demonstrated optical transitions in the UV-range from 200 to 800 nm and were measured with a UV-3600 UV–VIS–NIR Shimadzu spectrometer, operating from 190 to 3300 nm. AFM images were obtained with a Multimode Nanoscope IIIa (Digital Instruments – Veeco). Finally, Raman spectra were detected in the 50–800 $cm^{-1}$ UV-range using the 514.5 nm line of an Argon laser. All measurements were taken at room temperature.

* Corresponding author.
*E-mail address:* noelio@df.ufscar.br (N.O. Dantas).

0009-2614/$ - see front matter © 2010 Published by Elsevier B.V.
doi:10.1016/j.cplett.2010.09.035

## 3. Results and discussion

### 3.1. Optical absorption spectra

Figure 1 shows OA spectra from the pure, manipulated PZABP matrix (bottom line) and five samples containing ZnTe NCs with 480 °C post-growth annealing for 2, 4, 6 and 8 h. It is apparent that the PZABP substrate is transparent in the UV and visible ranges while ZnTe NCs absorb or emit light. Thus, this new matrix was essential to optically observe and control the growth of ZnTe NCs through OA spectra. It is possible to identify two distinct OA spectra bands for ZnTe dots grown in the Te doped PZABP matrix, both with and without thermal treatment. These bands are centered near 390 nm (3.18 eV) and 535 nm (2.33 eV), as shown by the trace labeled 0 h in Figure 1. This clearly shows that the cooling rate used was not high enough to impede $Zn^{2+}$ and $Te^{2-}$ ion diffusion and ZnTe NC growth. The band near 390 nm underwent a red-shift as annealing time increased. This is a clear signature of quantum confinement in dots of increasing size. However, the band at about 535 nm was not sensitive to the heat treatment. This absorption could be attributed to ZnTe clusters formed during melt cooling.

Average ZnTe dot sizes were determined by effective mass approximation (EMA) [16,17] where transition energy between electron and heavy-hole states was estimated by:

$$E_{conf} = E_g + \frac{h^2\pi^2}{2\mu R^2} - 1.8\frac{e^2}{\varepsilon R} \quad (1)$$

where $E_g$ is the bulk semiconductor energy gap, $\mu$ is the electron–hole reduced effective mass ($\mu_{ZnTe} = 0.1m_0 = 9.11 \times 10^{-32}$ Kg) and $R$ is the radius of the spherical confinement region. The third term is an estimate of electron–hole Coulomb interaction where $\varepsilon$ is the dielectric constant ($\varepsilon_{ZnTe} = 8.7$) [18]. Estimated average sizes ($R$) for the ZnTe QDs were 2.024 nm, 2.058 nm, 2.106 nm, 2.144 nm and 2.170 nm for 0, 2, 4, 6 and 8 h annealing times, respectively. If the third term in the EMA model is replaced by the bulk heavy-hole exciton binding energy ($E_{exZnTe} = 18$ meV) [18] it was observed that the structures formed over the new PZABP templates exhibited bulk properties beyond $R = 5.39$ nm.

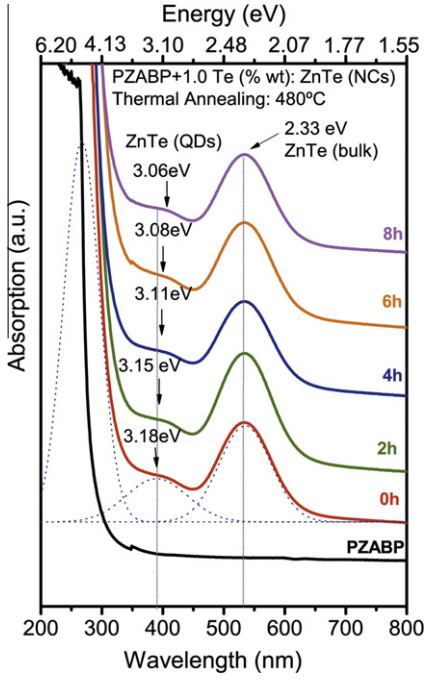


**Figure 1.** Room temperature OA spectra of ZnTe NCs grown on the UV-transparent PZABP template. Heat treatment time controls the average dot size in the sample. Even without annealing, this matrix displays two Gaussian optical bands.

### 3.2. AFM images

The left panels of Figure 2 show AFM images of ZnTe NCs grown in the new PZABP matrix with sizes proportional to the thermal treatment at 480 °C for 0 h (a), 6 h (b) and 8 h (c). A clear increase in dot size can be seen which is in agreement with the estimated values using the simplified EMA model and the OA energy peaks from the band at 390 nm (Figure 1). The right panels of Figure 2 show regions where the samples have ZnTe bulk-like properties in the new PZABP matrix.

### 3.3. Raman spectra

Finally, Figure 3 shows the Raman spectra for the same samples described in Figure 1 and for bulk ZnTe (top trace). The Raman transitions near 108, 216, 283, 323, 428, and 644 $cm^{-1}$ correspond, respectively, to the normal phonon modes: (i) second order transverse acoustic (2TA) [19–21], (ii) first order longitudinal optical (1LO) [2,11,12,19–21], (iii) second order longitudinal acoustic (2LA) [19–21], (iv) third order transverse/longitudinal optical coupled to the first order longitudinal acoustic (TO/LO + LA) [19,20] (v) second order longitudinal optic (2LO) [2,11,12,19,21,22], and (vi) third order longitudinal optic (3LO) [2,11]. It should be noted that this new PZABP matrix not only allows ZnTe NC growth but is also UV-transparent.

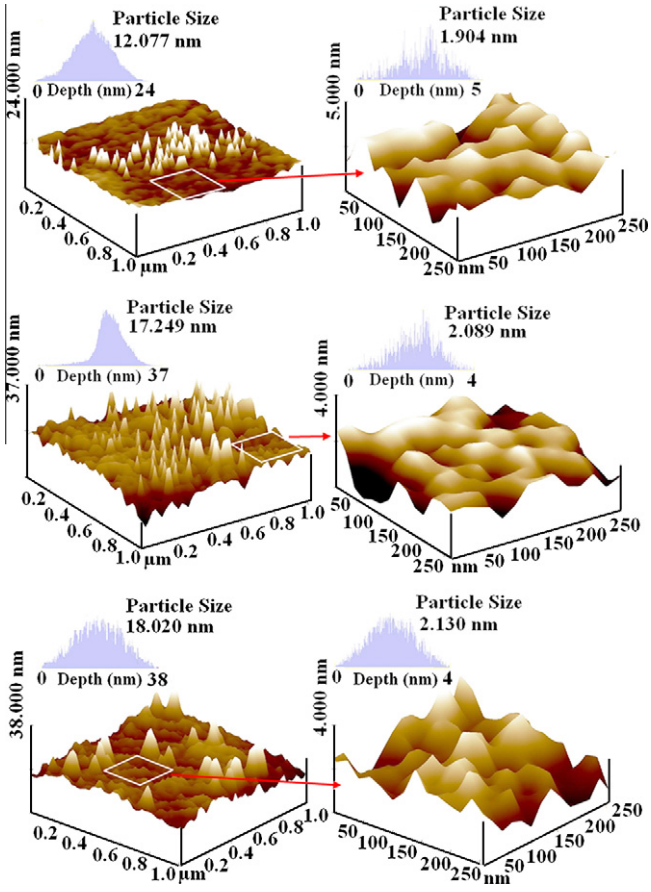


**Figure 2.** AFM images of ZnTe NCs grown on the new PZABP matrix, thermally annealed at 480 °C for (a) 0 h, (b) 6 h and (c) 8 h. These images illustrate dot morphology (left panels) and cluster regions (right panels) with ZnTe bulk-like properties.

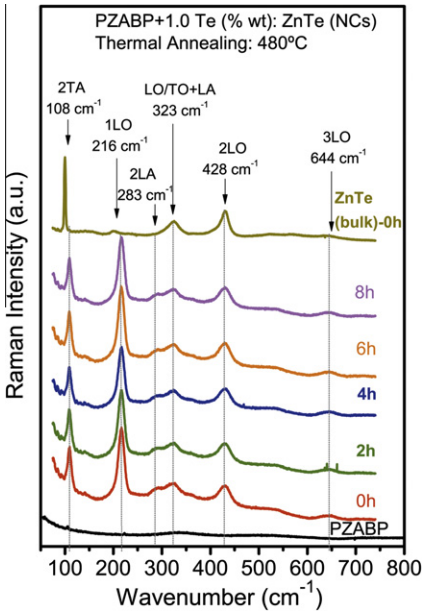


**Figure 3.** Room temperature Raman spectra from the same samples in Figure 1. The top trace shows the Raman spectrum for bulk ZnTe semiconductor crystals.

## 4. Conclusion

A new PZABP glass matrix was synthesized that allows ZnTe NC growth and is transparent for a wide range of electromagnetic radiation used in many experiments. NCs were synthesized by fusion and annealed post-growth to control average dot size. Sample properties were investigated by OA, AFM and Raman spectroscopy. An OA red-shift indicated a dot size increase proportional to annealing time. The samples displayed two distinct bands, one sensitive to heat treatment and the other with ZnTe bulk-like properties. Average dot size estimated with the EMA model agrees with the values determined from the AFM images. The Raman spectra gave strong evidence for ZnTe NC growth in the new PZABP glass matrix. It is hoped that these results may stimulate further research into new substrates that not only work in visible and broad-spectrum UV ranges, but also allow NC growth based on semiconductors with desirable properties for optoelectronic device applications.

## Acknowledgments

The authors are grateful for the financial support of the following Brazilian agencies MCT/CNPq, FAPEMIG, FAPESP and CAPES.

## References

[1] L. Zhao, B. Zhang, Q. Pang, S. Yang, X. Zhang, W. Ge, J. Wang, Appl. Phys. Lett. 89 (2006) 092111.
[2] K. Ersching, C.E.M. Campos, J.C. de Lima, T.A. Grandi, S.M. Souza, D.L. Silva, P.S. Pizani, J. Appl. Phys. 105 (2009) 123532.
[3] K.T. Yong, Y. Sahoo, H. Zeng, M.T. Swihart, J.R. Minter, P.N. Prasad, Chem. Mater. 19 (2007) 4108.
[4] S. Wu, Z.Q. Ren, W.Z. Shen, H. Ogawa, Q.X. Guo, Appl. Surf. Sci. 249 (2005) 216.
[5] S.H. Lee, Y.J. Kim, J. Park, Chem. Mater. 19 (2007) 4670.
[6] C.E.M. Campos, J.C. de Lima, T.A. Grandi, H. Höhn, J. Non-Cryst. Solids 354 (2008) 3503.
[7] H.S. Lee, H.L. Park, T.W. Kim, Appl. Phys. Lett. 92 (2008) 052108.
[8] Y. Yu, J. Zhou, H. Han, C. Zhang, T. Cai, C. Song, J. Alloys Comp. 471 (2009) 492.
[9] A.M. Salem, T.M. Dahy, Y.A. El-Gendy, Phys. B 403 (2008) 3027.
[10] S.S. Kale, R.S. Mane, H.M. Pathan, A.V. Shaikh, O.S. Joo, S.H. Han, Appl. Surf. Sci. 253 (2007) 4335.
[11] T. Wojtowicz et al., J. Korean Phys. Soc. 53 (2008) 3055.
[12] A. Abdi et al., Appl. Phys. Lett. 87 (2005) 183104.
[13] W. Szuszkiewicz et al., Mater. Sci.-Poland 26 (2008) 1053.
[14] J. Zhang, K. Sun, A. Kumbhar, J. Fang, J. Phys. Chem. C 112 (2008) 5454.
[15] U.V. Desnica, M. Buljan, I.D. Desnica-Frankovic, P. Dubcek, S. Bernstorff, M. Ivanda, H. Zorc, Nucl. Inst. Meth. Phys. Res. B 216 (2004) 407.
[16] L.E. Brus, J. Chem. Phys. 80 (1984) 4403.
[17] N.O. Dantas, E.S.F. Neto, R.S. Silva, D.R. Jesus, F. Pelegrini, Appl. Phys. Lett. 93 (2008) 193115.
[18] H.T. Grahn, Introduction to Semiconductor Physics, World Scientific Publishing, New York, 1999. p. 183.
[19] W. Sen, S. Wen-Zhong, O. Hiroshi, G. Qi-Xin, Chin. Phys. 12 (2003) 1026.
[20] J.C. Irwin, J. LaCombre, J. Appl. Phys. 41 (1970) 1444.
[21] R.L. Schimidt, B.D. McCombe, M. Cardona, Phys. Rev. B 11 (1975) 746.
[22] S. Nakashima, M. Jouanne, M. Scagliotti, C. Julien, M. Balkanski, J. Phy. C: Solid State Phys. 16 (1983) 3795.